ChemTexts (2019) 5:2
https://doi.org/10.1007/s40828-018-0077-9

LECTURE TEXT

Electrochemical promotion of catalytic reactions

R. Imbihl[1]

Received: 1 November 2018 / Accepted: 22 November 2018 / Published online: 4 December 2018

Abstract
An electrochemical promotion of heterogeneously catalyzed reactions (EPOC) became possible through the use of porous metal electrodes interfaced to a solid electrolyte. The EPOC effect has been demonstrated for more than 100 reaction systems. Surface science investigations showed that the physical basis for the EPOC effect lies in the electrochemically induced spillover of the transported ionic species onto the surface of the metal electrodes. This report summarizes the progress which has been achieved in the mechanistic understanding of the EPOC effect.

Keywords Heterogeneous catalysis · Solid electrolytes · Electrochemical promotion · Spillover

Introduction

Controlling heterogeneously catalyzed reaction by turning a knob on some control panel has always been a dream of chemical engineers. Of course, for systems in so-called "real catalysis" such a control has not been established up to now, but for a small number of experimental systems one came at least close to this idea. These reaction systems exhibit the so-called EPOC effect where EPOC stands for electrochemical promotion of catalytic reactions [1]. The EPOC effect is based on the use of solid electrolytes. In solid electrolytes, the electric current is transported via mobile ions while the electronic conductivity, in general, is negligible. As one attaches noble metal electrodes to a solid electrolyte in a reacting gas atmosphere, an electric current is flowing but one would not necessarily associate the electric current with a catalytic reaction which takes place on the surface of the metal electrodes. However, this is what happens in the EPOC effect. In these systems, one can change activity and selectivity of heterogeneously catalyzed reaction by varying the potential of an electrochemical cell. The effect thus combines two separate fields which are electrochemistry on one side, and heterogeneous catalysis and surface chemistry on the other side.

It was first realized by C. Wagner in 1970 that solid electrolytes interfaced with metal electrodes offer the possibility to control the chemical potential of a surface species by simply varying the electrical potential of the electrodes [2]. However, it was not until C. Vayenas found a very efficient realization by depositing porous noble metal electrodes (Pt, Ag, etc.) on a solid ionic conductor that this principle was demonstrated convincingly and that the effect was investigated systematically [3]. Up to now, the EPOC effect has been demonstrated for more than 100 reaction systems [1, 4].

The studies of the EPOC effect have been summarized in a number of excellent review papers and in several monographs [1, 4–9]. These reviews, of course, reflect the level of understanding at the time they were written. In the monograph of ref [1], the EPOC effect has been put into a broad perspective connecting the electrochemical promotion with promotion and spillover effects in heterogeneous catalysis. In a recent review by Vernoux et al., the emphasis was on recent developments such as the use of nano-dispersed metal electrodes [4]. The purpose of this paper is less to give a full account of the many different reaction systems where EPOC has been demonstrated but to show the basic experimental observations to the EPOC effect and to demonstrate the current level of mechanistic understanding [9].

✉ R. Imbihl
imbihl@pci.uni-hannover.de

[1] Institut für Physikalische Chemie und Elektrochemie, Leibniz-Universität Hannover, Callinstr. 3A, 30167 Hannover, Germany

Observation of electrochemical promotion

Solid electrolytes

Solid electrolytes are in fact a quite old phenomenon [4, 10]. The first observation dates back to 1834 when Michael Faraday observed that a PbF_2 crystal upon heating to 500 °C became electrically conducting. In that case, it is the F^- ion which becomes mobile at high enough temperature so that it can transport electric charge. Today, a large number of solid ionic conductors are known with the conducting anions O^{2-}, Cl^-, F^- and the conducting cations H^+, Li^+, Na^+, K^+, Ag^+ and Cu^+. The electric conductivity of solid electrolytes can even become comparable to that of liquid electrolytes. Some solid electrolytes exhibit a good conductivity at temperatures as low as − 30 °C while others such as the O^{2-}-conducting yttrium-stabilized zirconia (YSZ) require temperatures above 400 °C before they show substantial electric conductivity.

In a solid material, ions can only move only if vacant sites are available. In zirconia, one can create anionic vacancies by adding Y_2O_3 to ZrO_2 so that part of the Zr^{4+} is preplaced by Y^{3+}. An optimum ionic conductivity of O^{2-} ions is reached when about 10% Y_2O_3 are added to ZrO_2. In the Nernst lamp, this electric conductivity was exploited to create a light emitting device. Economically, this Nernst lamp was no success because the Edison lamp which appeared at about the same time was superior in its performance.

Solid electrolytes find applications in sensors, batteries and, last but not least, in fuel cells. In fuel cells, H^+-conducting polymers separate the cathodic and anodic half cells. A very small electronic conductivity of the H^+-conducting polymer is in that case essential because otherwise one would short circuit anode and cathode.

Solid electrolyte potentiometry (SEP)

In the following, we focus at the interface Pt/YSZ. We consider an electrochemical cell in which a YSZ tube separates two gas volumes with different oxygen partial pressures, $p(O_2, WE)$ and $p(O_2, RE)$, where the electric potentials are measured with two electrodes, a working electrode (WE) and a reference electrode (RE). With the following equilibrium:

$$O_2 + 4e^- \rightleftarrows 2O^{2-}, \tag{R1}$$

being established; the measured potential V_{WR} between the two electrodes, is given by the Nernst equation. V_{WR} is determined by the difference in chemical potential of gaseous oxygen, $\mu(O_2)$, between the inside and the outside of the tube:

$$\begin{aligned} V_{cell} &= 1/4F\left[\mu\left(O_2,\ WE\right) - \mu\left(O_2,\ RE\right)\right] \\ &= RT/4F\ \ln p\left(O_2, WE\right)/p\left(O_2, RE\right), \end{aligned} \tag{1}$$

with F representing the Faraday constant. The actual potentials are fixed by the electrochemical reactions at the three-phase-boundary (tpb) between solid electrolyte, metal electrode, and gas phase because it is there where the O^{2-} ions are discharged:

$$O^{2-} \rightleftarrows O_{tpb} + 2e^-. \tag{R2}$$

In other words, the open-circuit potential measures the activity of atomic oxygen, a_O, at the tpb. We obtain:

$$V_{WR} = RT/4F \ln {a_O}^2(\text{tpb, WE})/{a_O}^2(\text{tpb, RE}). \tag{2}$$

This use of solid electrolytes is called solid electrolyte potentiometry (SEP) [10–12]. In the automotive catalytic converter, for example, the so-called λ-probe measures the oxygen content in the exhaust gases to regulate the air/fuel ratio such that it is close to its optimum value. Otherwise, if the atmosphere is too oxidizing, NO is produced. If the atmosphere is too reducing, then CO and hydrocarbons are not burned to CO_2 and H_2O. This leaves a narrow range of the air/fuel ratio for avoiding contaminants which is called λ-window.

Experimental observation of EPOC

In the preceding section, we used the electrodes on YSZ to measure an electric potential that reflects the differences in the chemical potential of adsorbed oxygen on the two electrodes ("open-circuit potential"). If, instead, one applies an electric potential to the electrodes ("closed circuit potential") one arrives at the EPOC effect.

The total oxidation of ethylene to CO_2 and H_2O which proceeds according to

$$C_2H_4 + 3O_2 \rightarrow 2CO_2 + 2H_2O, \tag{R3}$$

is catalyzed by platinum. A typical experimental set-up for an EPOC experiment is displayed in Fig. 1a with a half-closed YSZ tube as catalytic reactor [13]. For the electrochemical measurements, a standard three-electrode set-up sketched in Fig. 1b is used. The catalytic reaction takes place on the surface of a porous Pt layer of roughly 3–30 µm thickness which also serves as working electrode (WE). The porous Pt electrodes are prepared by simply depositing a Pt paste with a brush followed by calcination and sintering. The chemical potential of oxygen outside the tube is fixed because of the constant oxygen partial pressure in air.

If we feed the reactants C_2H_4 and O_2 into the cell depicted in Fig. 1 and apply a voltage V_{WR} to the working electrode consisting of porous Pt, we observe a strong increase in the reaction rate as depicted in Fig. 2. The rate increase amounts to a factor of 26. Since a positive

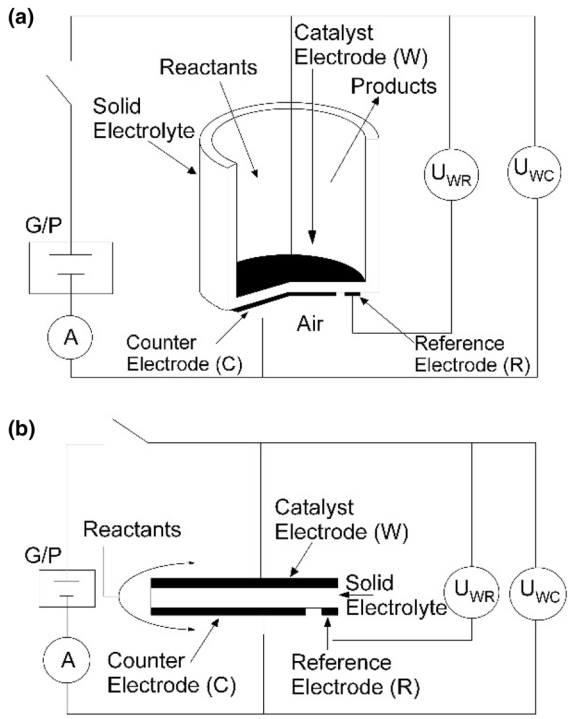

Fig. 1 Typical experimental set-up for EPOC experiments using a half-closed YSZ tube a reactor. The reactants are fed inside the tube where they react at the surface of the Pt working electrode (WE), whereas the reference electrode (RE) outside the tube is held in ambient air thus fixing the potential of the RE. A galvanostat/potentiostat controls the electric current/the electric potential. Reprinted with permission of ref. [5]

potential causes O^{2-} ions to be drawn to the WE, the measured increase in catalytic C_2H_4 combustion seems simply to be caused by the additional oxygen supply. Unexpectedly, the rate increase is strongly non-Faradaic by a factor of 74,000! One computes this number from the electric current, I, and from the electrochemically induced rate increase, $\Delta r = r - r_0$, where r is the rate with the potential on and r_0 the rate without an applied potential. By comparing the rate increase with the number of CO_2 molecules that would be generated if each transported O^{2-} ion would oxidize ethylene according to the stoichiometry of the reaction, one defines the Λ-factor or Faradaic efficiency (=NEMCA-factor in older publications). If we take for simplicity, catalytic CO oxidation where each transported O^{2-} ion would oxidize one CO molecule, one has.

$$\Lambda = \Delta r/(I/2F). \tag{3}$$

A Λ-factor of one would correspond to a Faradaic reaction. The strong non-Faradaicity of the reaction represents an unexpected and rather puzzling effect which was also responsible for first terming this effect as non-Faradaic electrochemical modification of catalytic (=NEMCA) effect. Later on, the more general expression EPOC effect was used. The highest Λ-factor of 3×10^5 was found for the $C_2H_4+O_2$ reaction on Pt/YSZ but also negative values are possible depending on whether a positive or negative applied electric potential causes a promotion or inhibition effect. The measured Λ-values accordingly cover a range from -1×10^4 to 3×10^5 [1, 6]. Defining a rate enhancement ratio, ρ, as

$$\rho = r/r_0, \tag{4}$$

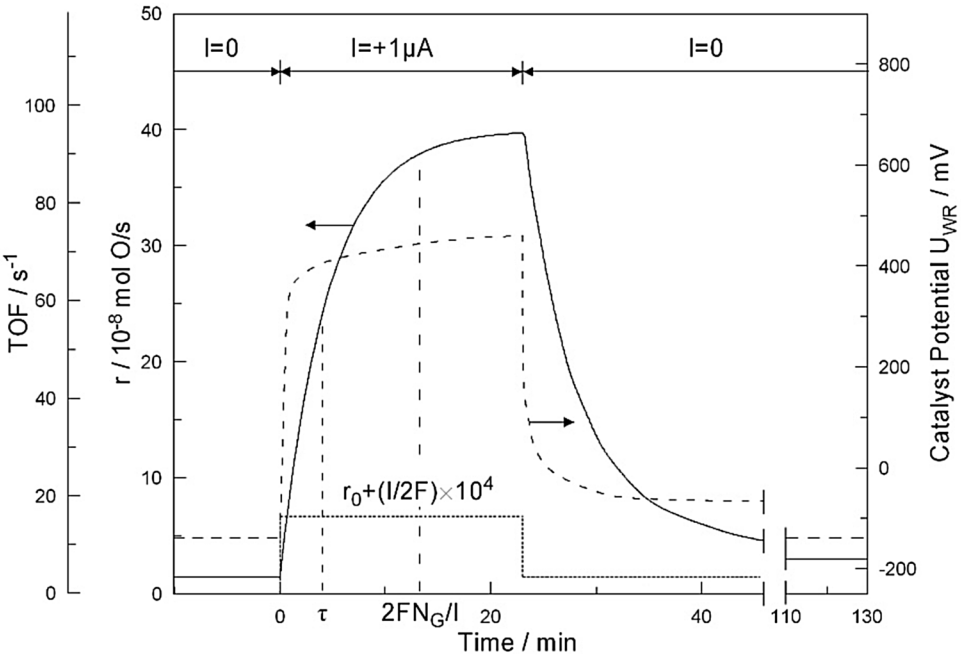

Fig. 2 Experiment demonstrating the electrochemical promotion of ethylene oxidation at a Pt/YSZ catalyst. The experiment is conducted in a particular way with a galvanostat controlling the electric current I. The response of the reaction rate and of the potential V_{WR} to an adjustment of an electric current I is shown. Experimental conditions: $T=643$ K, $p(O_2)=4.6\times10^{-2}$ mbar, $p(C_2H_4)=3.6\times10^{-3}$ mbar. Reprinted with permission of ref. [13]

where r_0 is the rate without electrochemical promotion, r the rate with electrochemical promotion, the reported ρ values range from 0 to 1400. Values below one indicate that a catalyst can also be poisoned by application of an electric potential [1, 4]. With regard to practical applications, the most significant effect in some reactions is perhaps not the electrochemically induced increase in catalytic activity but the change in selectivity.

Other reaction systems

The more than 100 reaction systems where the EPOC effect has been studied involve oxidation reactions of CO and organic molecules, NO reduction, hydrogenation and dehydrogenation reactions, isomerization and pure decomposition reactions [1, 5]. A few selected examples are shown in Table 1. Most of these reactions were investigated with noble metal catalysts such as Pt, Pd, Rh, and Ag serving as electrodes; in addition, less noble metals such as Ni and also the oxides IrO_2 and RuO_2 were studied. Besides the O^{2-} conducting system YSZ, the EPOC effect was shown to occur on different types of solid electrolytes: the Na^+-conducting β''-Al_2O_3 (β-alumina), the H^+-conducting Nafion membranes and the F^--conducting CaF_2. Also mixed ionic-electronic conductors such as TiO_2 were investigated. In this review we focus on the O^{2-}-conducting system YSZ/Pt.

Basic empirical relations

The EPOC effect naturally first raises the question after the electrochemical promotion mechanism and, second, after the explanation for the striking and puzzling non-Faradaicity of the promotion. The natural way to solve the mechanistic puzzle is to begin with gathering as many data as possible and then to establish empirical relations between the various quantities that play a role.

Work function change

Right from the beginning, it was evident that any activation of the catalyst by an electric current had to proceed via a modification of the catalytic surfaces, i.e. the electrode surfaces. A direct proof that the surfaces are modified was obtained in work function (WF) measurements made in situ during EPOC experiments. Defined as the energy required to transport an electron from a metal into the vacuum, in an energy diagram the WF is simply the energetic separation between the Fermi level and vacuum level. The WF is changed by adsorbates because the adsorbate complex consisting of adsorbed molecule/atom and the metal atoms of the substrate can be viewed as a dipole which, depending on the sign, increases or decreases the WF. In simple cases, i.e. assuming that the dipoles do not depolarize at high coverages and that no other changes occur on the surface besides changing the number of dipoles, the WF change, $\Delta\varphi$, is described by the Helmholtz equation:

$$\Delta\phi = N_a eP/\varepsilon_0, \tag{5}$$

where N_a is the number of adsorbed atoms/molecules per cm^2, e is the elementary charge, ε_0 the dielectric constant of the vacuum, and P the dipole moment of the adsorbate complex [19].

The latter is defined as the product of charge and separation distance of the charges δ^+ and δ^- of the dipole; the unit of P is 1 Debye = 3.36×10^{-3} Cm (C = Coulomb). The sign of the dipole moment is such that if the dipole is oriented outwards from the surface as in $O^{\delta-}$ $Me^{\delta+}$, then P is positive resulting in a WF increase. This equation assumes a constant dipole moment, i.e. it neglects depolarization effects which become significant at higher coverages.

The data in Fig. 3 display a 1:1 correlation between WF change and change in the applied potential V_{WR} (with respect to some reference value). Two different electrolytes, the O^{2-}-conducting YSZ and the Na^+-conducting β''-Al_2O_3 (β-alumina) have been employed investigating a number of different catalytic reactions. Clearly, a link is

Table 1 A few selected examples of reactions displaying an EPOC effect

Reaction	Catalyst	Transported ion	ρ_{max}	Λ_{max}	References
$C_2H_4 + O_2$	Pt/YSZ	O^{2-}	55	3×10^5	[13]
$CO + O_2$	Pt/YSZ	O^{2-}	6	2×10^3	[14]
$C_2H_4 + O_2$ epoxidation	Ag/YSZ	O^{2-}	30	300	[15]
$CO_2 + H_2$	Ru/YSZ	O^{2-}	1400	3×10^5	[4]
$NO + H_2$	Pt/β''-Al_2O_3	Na^+	30	n.d.	[16]
$CO + O_2$	Pt/CaF_2	F^-	2.5	200	[17]
1-C_4H_8 isomerization	Pd/Nafion	H^+	40	−28	[18]

A comprehensive list of reaction systems displaying EPOC up to 2001, one finds in ref. [1]

n.d. not determined

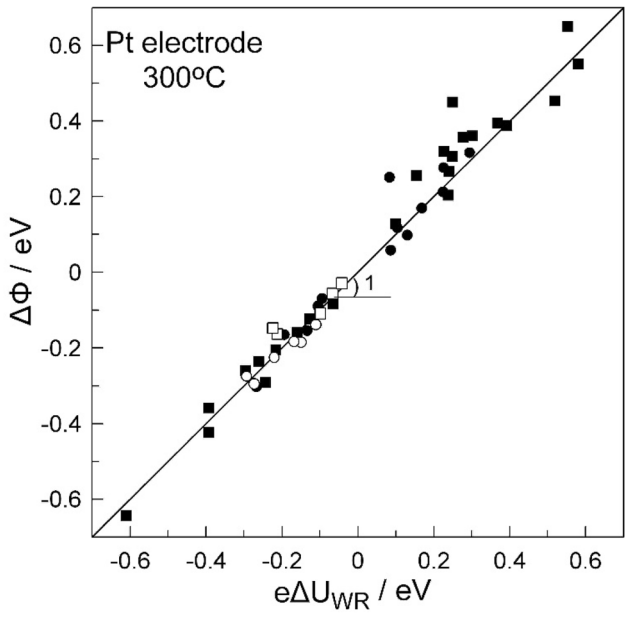

Fig. 3 Diagram demonstrating that the WF of a platinum electrode follows the electric potential V_{WR} with an approximate 1:1 relation. Different solid electrolytes are studied under open (open symbols) and closed circuit conditions (filled symbols). Circles: β''-Al_2O_3, $T=513$ K; squares: YSZ, $T=573$ K. Reprinted with permission of ref.[3]

thus established between the state of the surface and an electrochemical quantity. As has been shown in a detailed theoretical analysis, there is no strict equality $\Delta\varphi = V_{WR}$ that can be derived from the laws of physics [20]. This equality should, therefore, be viewed as an empirical relation which holds approximately over a range of ≈ 1 eV. In nearly all reviews of the EPOC effect by Vayenas et al., a "proof" for this equality has been presented but this "proof" is fundamentally flawed [9].

If we consider the interface Pt/YSZ, then the WF increase upon electrochemical pumping can be explained by oxygen spilling from the tpb where the ions are discharged onto the surface of the Pt electrodes:

$$O^{2-}_{YSZ} \rightleftarrows O_{tpb} + 2e^{-}, \tag{R4}$$

$$O_{tpb} \rightleftarrows O_{ad}. \tag{R5}$$

The spillover process for Pt/YSZ is depicted in Fig. 4. If we consider the spillover of oxygen onto the Pt surface of the working electrode as a similar process as the charging of a capacitor by an electric current I, then we can explain the time constant, τ, which appears in the rate curve of Fig. 2 in a simple way. The time constant should then obey the relationship:

$$t = 2FN_a/I, \tag{6}$$

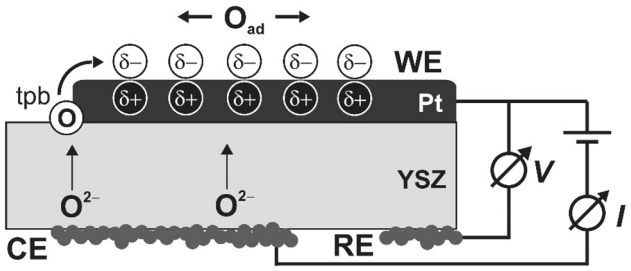

Fig. 4 Scheme demonstrating the electrochemically induced spillover of oxygen ions onto the surface of the metal electrode. The oxygen ions which are transported through the YSZ solid electrolyte are discharged at the tpb. The discharged oxygen species then migrate onto the surface of the Pt electrode

where N_a represents the number of adsorption sites per cm^2 on the electrode surface expressed in mol and I is the electric current, in the example of Fig. 2, $I=1$ μA [1, 6, 21]. Putting in reasonable estimates one obtains a time constant of a few minutes which is the time constant with which the rate curve in Fig. 2 changes upon switching on/off the electric potential.

As will be shown below, this electrochemically induced oxygen spillover has also been verified directly by experiment but a critical point is the following. In the above scheme, O_{ad} denotes oxygen atoms chemisorbed on the Pt surface but the question is can we simply equate the spillover oxygen species with oxygen being adsorbed from the gas phase or does the electrochemically induced spillover generate a species of its own? This will be the central question in the next chapter.

Dependence of rate increase on potential and of the Λ-factor on exchange current

For some reactions, the reaction rate was shown to increase exponentially with the applied electrochemical potential V_{WR} over a certain range of the applied potential [6]. This dependence can be brought into the form:

$$\ln(r/r_0) = a(V_{WR} - V^*_{WR})/kT, \tag{7}$$

where α and V^*_{WR} are adjustable parameters, specific for each reaction system. It turned out that very few systems exist where such an exponential dependence is really obeyed. In the vast majority of cases, the rate vs V_{WR} curve exhibits shapes which are quite different from a simple exponential dependence [1].

The exchange current is a measure of how fast ions are discharged at the interface metal/solid ionic described formally in the Butler–Volmer equation,

$$I/I_0 = \exp(\alpha_a F\eta/RT) - \exp(\alpha_c F\eta/RT), \tag{8}$$

where α_a and α_c denote the symmetry of the activation barrier with respect to initial/final state in the corresponding

potential diagram (usually around 0.5) [22]. I_0 is obtained by plotting the current I vs. the overpotential η in a so-called Tafel plot. The overpotential η is given by

$$\eta = V_{WR}(I) - V_{WR}(I = 0), \quad (9)$$

i.e. as the difference between the potential at chemical equilibrium and the potential when an electric current is flowing. A low I_0 means that the interface has to be strongly polarized to generate a certain electric current compared to a high I_0 which means low polarizability.

The relation,

$$|\Lambda| = 2Fr_0/I_0, \quad (10)$$

was derived in ref. [13] starting from the Butler–Volmer equation but this derivation contains flaws. Despite the missing theoretical justification, Eq. 10 works surprisingly well covering a range over five orders of magnitude of the Λ-factor. This equation relates the polarizability of the Pt/YSZ interface to the Λ-factor.

Mechanism of EPOC

The sacrificial promoter mechanism and the special spillover species

The big challenge of the EPOC effect is to explain the non-Faradaicity. The highest Λ-factor of 3×10^5 was found for the $C_2H_4 + O_2$ reaction on Pt/YSZ which means that each transported oxygen ion catalyzes the combustion of 100,000 ethylene molecules [13]. To explain the non-Faradaicity, the following mechanism was proposed by Vayenas et al. [1, 4, 6, 13]. The oxygen species which migrates from the tpb after discharge onto the Pt surface is not regular chemisorbed oxygen O_{ad}, but it is a different species carrying a certain negative charge δ^- so that one would formulate it as $O^{\delta-}$ with δ being between 1 and 2. In other words, a special spillover oxygen species should exist with properties distinctly different from those of chemisorbed oxygen, O_{ad}. This special spillover species is assumed to be strongly polar, i.e. it should exhibit a high dipole moment. Moreover, this species is supposed to have a strongly reduced reactivity compared to regular chemisorbed oxygen and it should be bonded more strongly to the surface than O_{ad}.

Exactly these properties are required to explain the non-Faradaicity of the promotion effect. Due to the high polarity of the spillover adsorbate complex, the spillover oxygen should modify the binding strength of co-adsorbed species via electrostatic through space dipole–dipole interactions. This causes a variation of the activation barriers of surface reactions, i.e. the kinetics of the catalytic reaction are modified. Since this special spillover species is less reactive than chemisorbed oxygen, it can influence the surface reaction while being very slowly consumed itself. This special spillover species thus acts very similar to a classic electronic promoter in catalysis, for example, like potassium in ammonia synthesis via Haber–Bosch which is presumably present on the surface as an ionic species K^+. This mechanism has accordingly been termed "sacrificial promoter mechanism" by Vayenas et al., since, in contrast to a classical promoter, the promoting species is consumed slowly here by the reaction. In this scheme, the non-Faradaic nature is a natural consequence of the promoter role of the spillover species.

The proposed "sacrificial promoter mechanism" is a very ingenious construction which is in itself consistent but the decisive questions are whether the postulated special spillover species can be verified in experiment and whether it has the required properties.

UHV-type studies

Identification of spillover species

Using X-ray photoelectron spectroscopy (XPS), one can characterize the different oxygen species on Pt by their O1s binding energy (BE) [23]. Neglecting the weakly bonded molecular species, one has essentially two different oxygen species in the system Pt/O: chemisorbed oxygen, O_{ad}, formed by dissociative adsorption of O_2 from the gas phase and oxidic oxygen, O_{ox}, which is the oxygen in Pt bulk compounds such as PtO_2 or Pt_2O_3 or in Pt surface oxides. Pt oxides as bulk compound are thermodynamically stable only at elevated pressures (> 1 mbar). The spectroscopic signature of an oxidic Pt species is a shift in the Pt 4f BE. Chemisorbed oxygen is very reactive oxidizing, for example, adsorbed CO rapidly to CO_2. In addition, an oxidic species might exist as a result of contamination. For example, the very stable and unreactive compound SiO_x (x close to 2) is very often found on Pt surfaces since Si is a typical contamination of Pt metal.

XPS measurements of Pt/YSZ are not trivial because porous Pt is partially transparent to X-rays so that part of the signal stems from the underlying YSZ substrate. In XPS the binding energy is referenced to the Fermi level. XPS measurements are typically conducted with the WE being grounded. Problems can, therefore, arise if not all parts of the Pt electrode are electrically connected and, therefore, at ground potential or if part of the signal stems from the underlying YSZ which is not at ground potential.

To have well-defined conditions, model systems for the Pt/YSZ catalysts with porous Pt layers were constructed employing optical lithography. These are the planar microstructured Pt/YSZ samples depicted in Fig. 5. They have the additional advantage that the tpb Pt/YSZ/gas phase is directly accessible to experimental observation. With high-intensity synchrotron radiation, spatially resolved

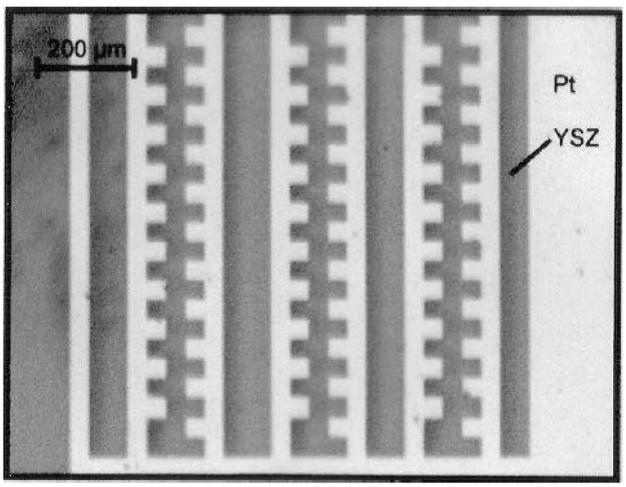

Fig. 5 Optical micrograph of a microstructured Pt film of 500 Å thickness on single-crystalline YSZ. This microstructure is used for the XPS experiment displayed in Fig. 6

measurements are feasible that also provide local spectroscopic information [24]. In the microstructure depicted in Fig. 5, local XP spectra were taken from a spot of 0.2 µm diameter on the Pt electrode about 20 µm away from the tpb [25].

As demonstrated by the O1s spectra in Fig. 6a, after some cleaning cycles oxygen is left on the surface. The signals at 531 and 534 eV are attributed to SiO_2 which is more or less inert under the conditions chosen here. Introducing gaseous oxygen causes the growth of an O1s component at 530.4 eV representing the well-known species of chemisorbed oxygen on platinum (Fig. 6b). Closing the oxygen valve, one observes the removal of this species within a few minutes due to so-called clean-off reactions of chemisorbed oxygen with CO and H_2 from the residual gas. As we now apply a positive potential of 1.1 V, the rapid growth of an O1s signal is seen whose area is 1.5 larger than the amount adsorbed from the gas phase. Important, the same peak position as with O_2 is found as shown in Fig. 6c. This experiment demonstrates that, first of all, electrochemical pumping causes a spillover of oxygen from YSZ onto the Pt surface. Second, the spillover oxygen species is clearly identical with oxygen from the gas phase. The Pt 4f signal displays no change upon electrochemical pumping thus excluding the formation of an Pt oxide [25].

The spectra in Fig. 6 do not show any sign of a special spillover species corresponding to a charged $O^{\delta-}$ species. The absence of this species is what we expect from physical intuition because as soon as the oxygen jumps from the tpb onto the Pt surface, it should lose its memory of where it originally came from. In a preceding XPS study of Pt/YSZ in UHV, an O1s component at 528.8 eV appeared upon electrochemical pumping which is different from the BE of usual

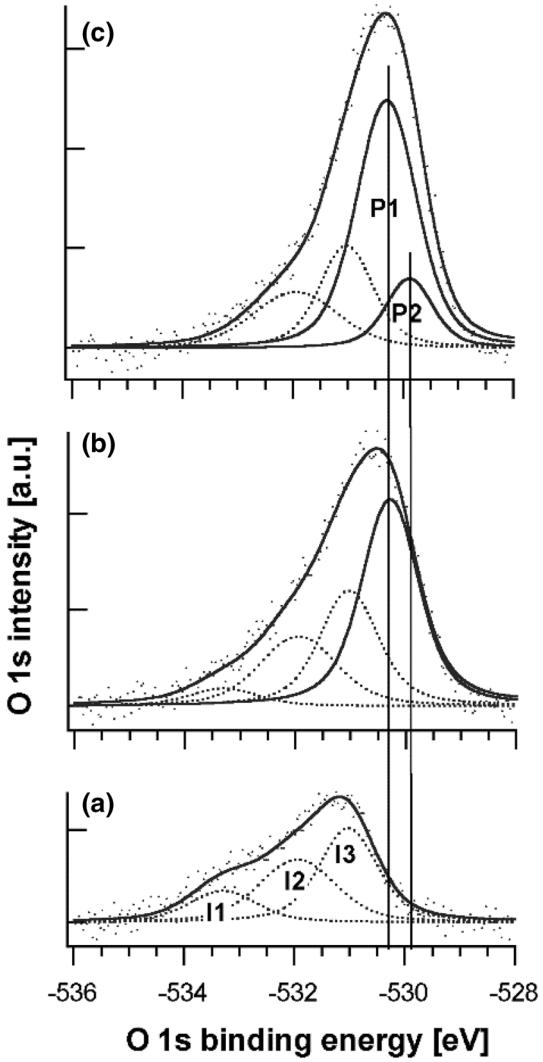

Fig. 6 Characterization of the electrochemically induced oxygen spillover species of a Pt/YSZ catalyst by photoelectron spectra of the O1s region. The spectra are taken from $a \sim 0.02$ µm^2 spot on the microstructured Pt surface displayed in Fig. 5: **a** the residual O1s spectrum after the cleaning cycles with I1-I3 representing oxygen components attributed to contaminants like SiO_2; **b** the O1s spectrum measured in O_2 atmosphere ($p(O2) = 1 \times 10^{-6}$ mbar); **c** the O1s spectrum obtained during electrochemical pumping in vacuum with $V_{WR} = 1.1$ V. P1 and P2 are the components which are formed by adsorption from the gas phase and by electrochemical pumping. The fitting components of the residual oxygen are shown with dashed lines. Photon energy = 643.2 eV, $T \approx 350$–400 °C. From ref. [25]

chemisorbed oxygen at 530 eV [26]. Accordingly, this species was assigned to the postulated special spillover species of oxygen. This result is thus in contradiction to data shown in Fig. 6 but since these measurements have been conducted with an integral XPS and with a porous Pt electrode artifacts such as local charging of the Pt layer or contributions from the underlying YSZ may be responsible for the appearance of the new state. Later on, XPS measurements carried out with a porous Pt electrode in fact confirmed that the oxygen

spillover species on porous Pt is also identical with regular chemisorbed oxygen [27].

Several other techniques have been applied to characterize the oxygen spillover species on Pt/YSZ. In thermal desorption spectroscopy (TDS), the desorption of an adsorbate into the gas phase is followed as the sample is heated up in vacuum with a linear heat ramp; the area under the desorption trace is proportional of the coverage and the temperature of the desorption maxima is a measure for the binding strength of the adsorbate to the surface. It was shown that electrochemical pumping leads to the filling of a lower lying adsorption state of oxygen, but the states in TDS are not specific enough to deduce the existence of a special spillover species [1, 9, 28]. What these experiment, however, demonstrated was that electrochemical pumping is able to produce much higher oxygen coverages than by adsorption from the gas phase.

Cyclic voltammetry (CV) is an electrochemical characterization method which in a way is similar to TDS in surface science because the oxidation/reduction of species upon cyclic variation of the electrode potential gives rise to characteristic peaks in the electric current [22]. Also, here a new state was found upon electrochemical pumping of Pt/YSZ but subsequent studies demonstrated that the new state attributed to a special oxygen spillover species might have its origin in a contamination of the surface [29, 30].

Spatially resolved techniques

According to the spillover picture, the oxygen species after discharge at the tpb spreads out onto the Pt surface. With spatially resolving techniques, one should be able to image this spreading process but the problem is that with porous Pt electrodes the tpb is obscured from observation. However, with planar microstructure Pt electrodes of the type displayed in Fig. 5, this imaging of the spillover process should be possible.

For imaging dynamic variations of an adsorbate distribution which proceed on a macroscopic (μm) scale, photoelectron emission microscopy (PEEM) is an ideal tool [24, 31]. This technique is non-destructive and the PEEM can be operated as an in situ method for $p < 10^{-3}$ mbar. PEEM is based on the photoelectric effect. If the sample is illuminated with photons from a D_2 discharge lamp (5.5–6 eV photon energy), then photoelectrons are ejected which can be imaged with an electrostatic three-lens system onto a phosphorous screen from where the images are recorded with a video camera and digitized. With a conventional instrument typically, a spatial resolution of 0.1–1 μm is reached. PEEM images primarily the local work function (WF). Areas with a high WF appear dark in PEEM, whereas areas with a low WF show up as bright regions in PEEM. Since adsorbed oxygen, owing to its high electronegativity, strongly increases the WF of metal surfaces (0.5–1 eV), oxygen-covered areas appear dark in PEEM.

As expected, the porous Pt film of Pt/YSZ became uniformly dark in PEEM upon electrochemical pumping with a positive potential but, different from expectations, also the microstructured planar Pt films only showed a uniform darkening as the film was set to a positive potential. The puzzle why the expected spreading via a diffusional front was not seen was solved as scanning electron microscopy showed the presence of numerous small pores in the Pt layer with a pore size below the resolution of PEEM [32]. One can prepare Pt films without pores by applying laser deposition of Pt followed by annealing thus creating a dense (111) oriented Pt film. On such a sample one can observe the diffusional spreading of spillover oxygen away from the tpb as demonstrated by the PEEM images in Fig. 7 [32]. From the evolution of the intensity profiles, one extracts an oxygen diffusion concentration gradient $D_O = 9 \times 10^{-4}$ cm^2 s^{-1} for $T = 670$ K [32]. This value which represents macroscopic diffusion is about four to five orders of magnitude larger than the values obtained for Pt(111)/O with techniques analyzing microscopic diffusion, i.e. STM, field electron microscopy (FEM) and quantum chemical calculations [33–36]. In the above analysis, Fickian diffusion was assumed but, in particular at high adsorbate coverages, diffusion is no longer Fickian because energetic interactions come into play. Fickian diffusion is valid if no energetic interactions between the diffusing particles exist as it is the case in an ideal gas. Repulsive interactions between adparticles are known to decrease the activation barrier for diffusion thus accelerating surface diffusion. Due to a more dense packaging, high coverages lead to strong repulsive interactions. This effect might be responsible for diffusion in the Pt/YSZ experiment at high-oxygen coverages being much faster than diffusion measured at much lower oxygen coverages on single-crystalline surfaces [9].

The relatively high diffusivity of spillover oxygen is also essential for porous Pt layers being so effective in the electrochemical promotion of catalytic reactions. First, such catalysts due to their porous nature exhibit a much larger area accessible to the gas phase than the geometric area. Second, they possess a long tpb which has been estimated based on electron microscopy and CV to be in the range of several 10^3 m/cm^2 for typical Pt/YSZ catalysts [1]. Finally, oxygen diffusion is fast enough so that spillover oxygen can reach the outer layers of the about 3–30-μm-thick Pt electrodes. Without the latter property, no WF change upon electrochemical pumping would be detected in PEEM or with a Kelvin probe.

With scanning tunneling microscopy, the group of Vayenas succeeded to show that electrochemical pumping caused the appearance of a (12×12) structure on a Pt(111) single crystal which had been interfaced to YSZ [37]. Also here,

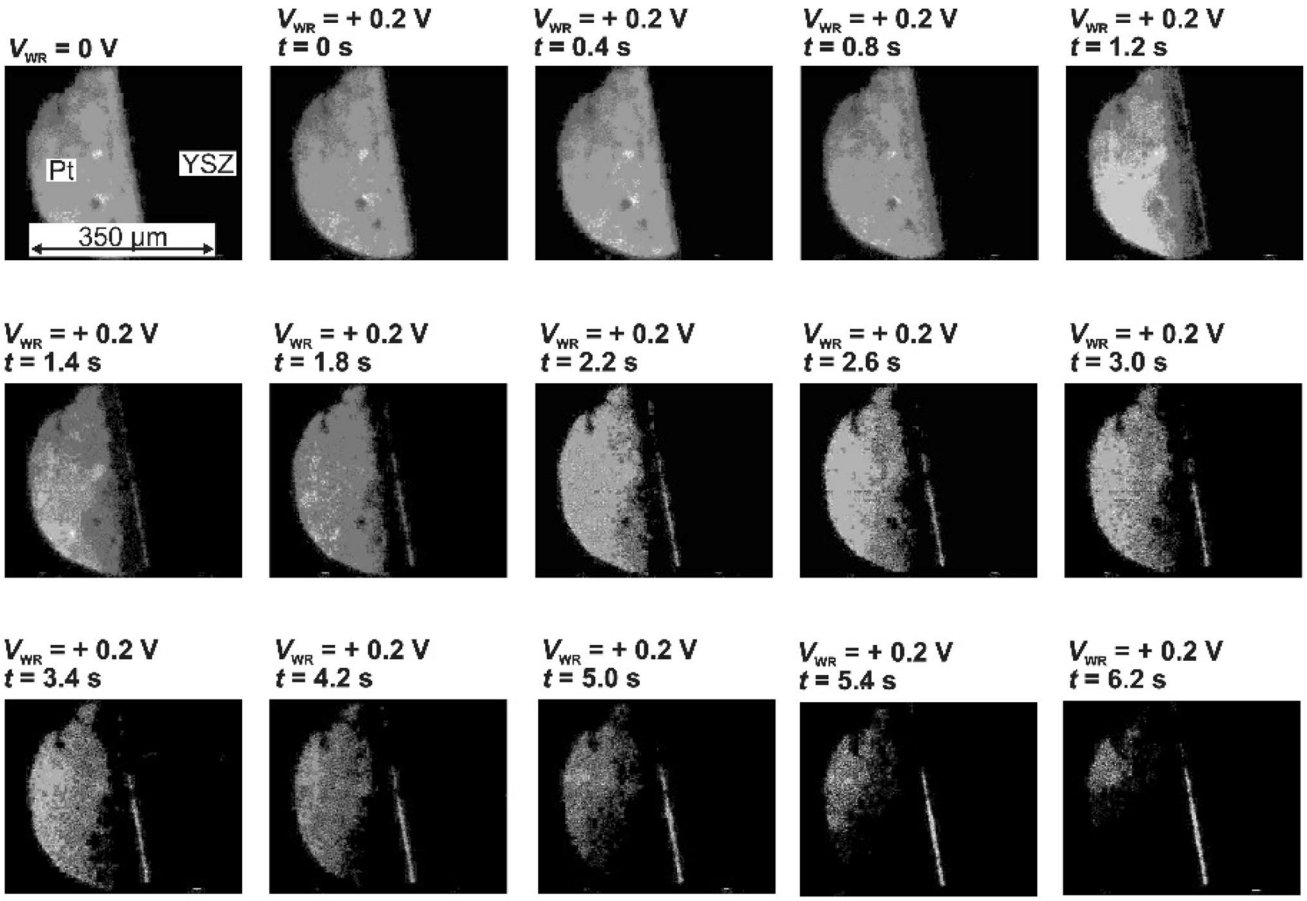

Fig. 7 Sequence of PEEM images showing the spreading of spillover oxygen on a dense Pt electrode during anodic polarization with $V_{WR}=+0.2$ V at $T=670$ K. The first image with $V_{WR}=0$ V shows the tpb with the Pt electrode on the left and the YSZ electrolyte on the right. Oxygen adsorbed on Pt is imaged as dark area. From ref. [32]

similar to CV, the origin of the (12×12) is likely to lie in contaminants because no (12×12) structure is known for the pure system Pt(111)/O.

Promotion by alkali metals

Alkali metals play as so-called electronic promoters an important role in a number of industrially important reactions such as ammonia synthesis via Haber–Bosch or the Fischer–Tropsch synthesis of hydrocarbons and higher alcohols [38–40]. Beginning with the early work of Langmuir, numerous surface science studies focused on the adsorption of alkali metals (AMs) on transition metal surfaces. The AMs lead to a drastic decrease of the work function by as much as 5 eV because they donate their valence electron almost completely to the metal. Adsorbed AMs can induce surface reconstructions, cause the formation of surface alloys, and change the binding of co-adsorbed atoms and molecules.

When metal electrodes are interfaced to an alkali ion conducting solid such as the Na^+-conducting β''-Al_2O_3, through variation of the potential V_{WR}, the metal surface can be reversibly covered with alkali metal according to the reaction $Na^+ + e^- \rightleftarrows Na$. Since the first studies in 1991, the EPOC effect for alkali ion conducting solid electrolytes has been investigated for more than a dozen of different reaction systems involving catalytic CO oxidation, NO reduction, selective hydrogenation of alkines, and the epoxidation of alkenes [41–44]. For AM-conducting ionic solids, the electrochemical promotion is supposed to be very similar to the classical use of AM's in heterogeneous catalysis. An additional degree of freedom is provided because the amount of the alkali promoter can be controlled via an electric potential. Different from the "sacrificial promoters" AMs are not consumed by the reaction. This is reflected in a Λ-factor which is infinite or at least very large. Depending on the reaction system, AMs may not necessarily be promoters but they may also act as a catalytic poison. Consequently, one finds rate enhancements with r/r_0 varying between zero and 30 [1].

The EPOC studies of the electrochemical promotion with AM's were pioneered by the groups of R. Lambert

in Cambridge and by C. Vayenas in Patras. The variation of selectivity and activity as the concentration of an alkali promoter is electrochemically controlled was investigated with a number of technologically important catalytic reactions: in environmental catalysis with reactions comprising NO reduction and CO oxidation, with the selective hydrogenation of alkines, with the Fischer–Tropsch synthesis, and with the epoxidation of alkenes. For most of these reaction systems, a promotion effect with alkali metals was already known from earlier studies without electrochemical promotion.

The main surface analytical technique for studying the EPOC effect with AMs was XPS. This technique in nearly all cases was not applied in situ but after exposure to reaction conditions. A direct proof for the electrochemically induced spillover of alkali metal was obtained with scanning photoelectron microscopy (SPEM) using synchrotron radiation. Williams et al. demonstrated that upon electrochemical pumping of a Pt/K–β″-Al_2O_3 catalyst with a negative potential, spillover potassium spreads out uniformly on the Pt surface [45].

The systems for which the effect of the alkali metal promotion is probably best understood are the NO-reducing reactions. As demonstrated by Fig. 8 for the NO + CO reaction, the N_2 production rate raises with increasing negative potential, i.e. with increasing sodium coverage. Simultaneously with N_2 production, also the CO_2 rate grows while the N_2O formation rate decreases [39]. Clearly, with rising Na coverage the selectivity shifts towards N_2 formation. The

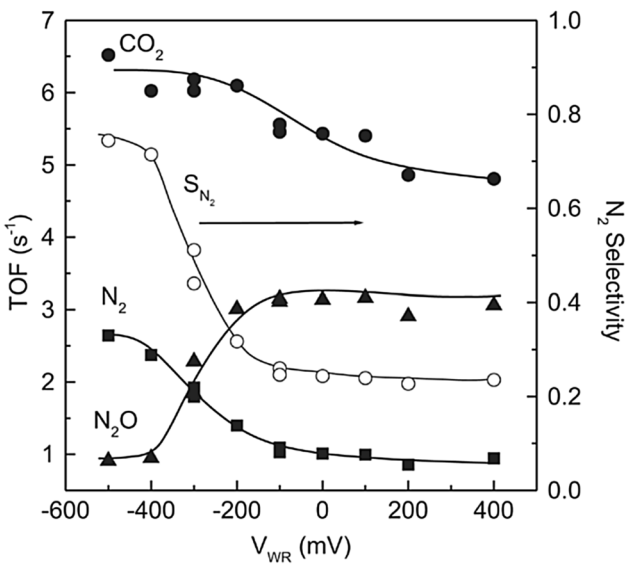

Fig. 8 Electrochemical promotion in the NO + CO reaction over at Rh/β″-Al_2O_3 catalyst. The CO_2, N_2, and N_2O production rates are shown as a function of the applied potential V_{WR}. Experimental conditions: $p(NO) = p(CO) = 1 \times 10^{-2}$ mbar, $T = 580$ K. Reprinted with permission of ref. [44]

increasing efficiency in NO-reducing reactions seen with rising alkali metal coverage can be summarized by stating that the alkali promoted Pt catalyst becomes similar to Rh. Rh dissociates NO far more easily than Pt and for this reason it is used in the automotive catalytic converter to remove NO_x emissions from the exhaust gases. Mechanistically, the effect of the AM can be attributed to enhanced NO dissociation which typically is the rate-limiting step in NO-reducing reactions:

$$NO_{ad} + * \rightarrow N_{ad} + O_{ad}, \quad \text{(R6)}$$

where * denotes a vacant adsorption site. The effect of the AM is the donation of electrons into the anti-binding 2π*-orbital of NO, thus weakening the intramolecular NO bond and facilitating dissociation.

Alkali metals are highly reactive and mobile. It is, therefore, unlikely that they are present in their metallic form under reaction conditions. Post-reaction XPS experiments in fact demonstrated the formation of stable alkali metal compounds, i.e. of compounds such as Na_2CO_3 $NaNO_3$, KNO_3 or KNO_2.

Thermodynamic driving force

A solid basis for understanding the electrochemically induced spillover of oxygen onto the surface of metal electrodes is provided by chemical thermodynamics. One assumes that chemical equilibrium is established—a simplification which will not be fulfilled if a catalytic reaction is involved. For a full discussion, the reader is referred to ref. [46]; here only the main arguments will be reproduced.

Following Eqs. R4 and R5, the discharge of oxygen ions at the tpb generates an atomic oxygen species, O_{tpb}, which can spill over onto the Pt electrode. On Pt chemisorbed oxygen, O_{ad} is formed. We assume that the equilibria R4 and R5 hold and we consider a standard three-electrode set-up of the type sketched in Fig. 1b with all electrodes made of Pt and YSZ as solid electrolyte. Introducing the electrochemical potential, $\tilde{\mu}_i$, defined by

$$\tilde{\mu}_i = \mu_i + z_i F \varphi, \quad (11)$$

with ϕ representing the Galvani potential (the inner potential) and z_i being the charge of the ionic species i, reaction R4 can be formulated as a chemical equilibrium:

$$\tilde{\mu}_{O^{2-}}(YSZ) = \mu_O(tpb) + 2\tilde{\mu}_{e^-}(Pt). \quad (12)$$

The quantity $\tilde{\mu}_{e^-}$ is the Fermi level determined by the electrochemical potential of electrons as $\tilde{\mu}_{e^-} = \mu_{e^-} - F\varphi$. Separating electrical and chemical contributions, the potential drop across the Pt/YSZ interface amounts to

$$\varphi(Pt) - \varphi(YSZ) = 1/2F\left[\mu_O(tpb) - \mu_{O^{2-}}(YSZ) + 2\mu_{e^-}(Pt)\right]. \quad (13)$$

According to this equation, the chemical potential of oxygen at the tpb follows directly the drop of the electrical potential across the interface because both, $\mu_{O^{2-}}$(YSZ) and μ_{e^-}(Pt), are constant as long as no change in the material composition occurs. If we first consider the potential difference between WE and RE for open-circuit conditions by setting $I=0$, then Eq. 12 becomes

$$\begin{aligned} V_{\mathrm{WR}}(\mathrm{I}=0) &= \varphi(\mathrm{Pt},\ \mathrm{WE}) - \varphi(\mathrm{Pt},\ \mathrm{RE}) \\ &= 1/2F\left[\mu_{\mathrm{O}}(\mathrm{WE},\mathrm{tpb}) - \mu_{\mathrm{O}}(\mathrm{RE},\ \mathrm{tpb})\right]. \end{aligned} \tag{14}$$

Furthermore, we assume that the adsorbed atomic species is in adsorption/desorption equilibrium with oxygen in the gas phase according to $2\mathrm{O}_{\mathrm{ad}} \rightleftarrows \mathrm{O}_2$. Then we have $\mu_{\mathrm{O}} = 1/2\mu_{\mathrm{O}_2}$ (gas). One obtains the Nernst equation in the form:

$$V_{\mathrm{WR}}(I=0) = 1/4F\left[\mu_{\mathrm{O}_2}(\mathrm{WE},\mathrm{gas}) - \mu_{O_2}(\mathrm{RE},\ \mathrm{gas})\right]. \tag{15}$$

With a non-zero electric current, electrode kinetics come into play. Neglecting the Ohmic *IR* drop inside the solid electrolyte, the overpotential, η, defined in Eq. 9 transforms Eq. 14 into

$$\eta = 1/2F\left[\mu_{\mathrm{O}}(\mathrm{WE\ tpb},I) - \mu_{\mathrm{O}}(\mathrm{WE\ tpb},I=0)\right]. \tag{16}$$

The overpotential not only contains the activated charge transfer across the Pt/YSZ interface but also reflects all kind of mass transport limitations and kinetic barriers. Equation 16 states that by changing V_{WR}, i.e. the overpotential, one can control the chemical potential of chemisorbed oxygen on the surface of the working electrode. The electric potential directly only influences the charged species, O^{2-}, but, since the charged species via R4 and R5 is in equilibrium with the atomic species on the tpb and on the WE, changes in V_{WR} automatically transform into a shift of the chemical potential of chemisorbed oxygen. This electrochemically induced variation in the chemical potential of oxygen is the thermodynamic driving force for the spillover of oxygen onto the surface of the working electrode.

Using $\mu_{\mathrm{O}_2} = \mu^0_{\mathrm{O}_2}(T) + RT\ln\frac{p_{\mathrm{O}_2}}{p^0}$, one obtains the Nernst equation in the form:

$$V_{\mathrm{WR}} = \frac{RT}{4F}\ln\frac{p_{\mathrm{O}_2}(WE)}{p_{\mathrm{O}_2}(RE)}, \tag{17}$$

which is identical with Eq. 1. This equation predicts that a small change in the potential V_{WR} corresponds to a huge difference in oxygen pressure on both sides of the solid electrolyte. For a temperature of 400 °C and a potential $V_{\mathrm{WR}}=0.5$ V, one obtains 15 orders of magnitude for the pressure ratio. Setting $p\mathrm{O}_2(\mathrm{reference}) = 10^{-10}$ mbar, a pressure of 100 bar at the WE results. This high virtual oxygen pressure does only partially translate into a correspondingly high chemical potential on the metal electrode because otherwise the Pt would spontaneously transform into Pt oxide. A Pt oxide at the Pt/YSZ interface has been detected but the amount is small and varies strongly with the experimental conditions [47].

Rules of promotion

In an attempt to summarize the experimental results of different reaction systems in EPOC and to be able to predict the behavior of new systems, "rules of promotion" have been formulated [1, 4, 48]. In particular, the rules should tell one, whether a positive or negative potential should be beneficial for promoting a certain reaction. Assuming that the equality $\Delta\varphi = V_{\mathrm{WR}}$ holds (which actually is only an approximate empirical relation and not generally valid), the rules have been formulated with respect to the work function and not with respect to the choice of the potential V_{WR}. Depending on the behavior of the reaction rate r upon variation of φ ($=V_{\mathrm{WR}}$), four different cases are distinguished:

i. the rate r increases with the work function φ, that is $\partial r/\partial\varphi > 0$, called "electrophobic behavior"
ii. the rate r decreases with the work function φ, that is $\partial r/\partial\varphi < 0$, called "electrophilic behavior"
iii. the rate exhibits a relative maximum with respect to variation of φ, called "volcano-type behavior"
iv. the rate exhibits a relative minimum with respect to variation of φ, called "inverted volcano-type behavior"

One notes that this classification replaces the simple exponential dependence of the rate upon variation of V_{WR} in Eq. 7 which initially had been assumed to be valid. With respect to the adsorbates, one distinguishes between acceptors A associated with a WF increase and donators connected with a WF decrease. Following this distinction and the above classification in four types of behavior, simple rules have been formulated such as "strong adsorption of A causes electrophobic behavior", i.e. the rate increases with the WF ($\partial r/\partial\varphi > 0$). A certain rationalization can be found in surface science in the well-studied co-adsorption behavior of reactants. A donor, i.e. an adsorbate which provides electrons like an alkali metal will weaken the bonding of a co-adsorbed acceptor like NO because electrons are put into antibonding molecular orbitals. The problem is the following. The WF is a rather unspecific property summarizing all effects of electron redistribution on the surface including surface reconstruction, co-adsorption and depolarization effects. Different species of the same adsorbate can cause opposite WF changes, for

example, chemisorbed oxygen and oxidic oxygen on some metals. Practically, no information from in situ studies is available showing what species are actually causing the WF changes summarized in the diagram of Fig. 3. In all these systems, several species and not just the spillover species will be present on the surface. Thus, with exception of the alkali promoters perhaps, one cannot sure about what species are responsible for the WF changes induced by the potential V_{WR}.

It is of course perfectly legitimate to formulate empirical rules but without substantiating these rules by a mechanistic understanding, these rules are not really satisfactory. These difficulties become evident as the same reaction system depending on the reaction conditions belongs to three different classes of the promotion rules, e.g. C_2H_4 oxidation on Pt or NH_3 synthesis over Fe [4]. A more general remark is that it is quite dangerous to relate the catalytic activity to a single parameter, the work function. In today's theories, the energetic position of the d-band center and the electronic states near the Fermi level often play the role as descriptors of catalytic properties of a metal but an approach which merely uses the WF is apparently inadequate [49].

Pressure and material gap problems

What is the pressure and material gap?

Definition

This term describes the difference between single-crystal experiments conducted at 10^{-10} mbar in an UHV chamber and so-called "real catalysis" which operates with complex mixtures of substances typically in a pressure range $\approx$ 1–100 bar [50–52]. A problem arises when one tries to explain heterogeneous catalysis using the results of surface science because this means that one extrapolates the findings obtained at 10^{-10} mbar to atmospheric pressure. This approach is in general not valid for several reasons. For thermodynamic reasons, certain phases which are essential for the catalytic functioning may develop only above a certain pressure threshold so that UHV studies will have no chance of detecting such a phase. In kinetics, a certain pathway which plays no role at low p may become dominant at high because the high coverages enforced by a high pressure will alter the kinetic barriers. Most importantly, structure and composition of a catalyst in operation will be different from the catalyst at 10^{-10} mbar because of dynamic restructuring processes and of chemical transformations. In other words, a catalyst in operation is a "living catalyst". Finally, an important difference between high- and low-pressure studies of catalysis is that at high pressure ($> 10^{-3}$ mbar) mass and heat transport limitations come into play. Concentration gradients in the gas phase may develop and the reaction may no longer be isothermal.

Strategies to bridge the pressure and material gap

The most important strategy to bridge the pressure gap is certainly the use of in situ methods at high pressure because only then one has the guarantee that spectroscopic or microscopic measurements actually represent the active state of the catalyst. With conventional spectroscopies, the use of electrons is restricted to $p < 10^{-3}$ mbar but applying differential pumping this range can be extended to $\approx$ 1–10 mbar. With photons practically no upper pressure limit exists suggesting, for example, the use of infrared spectroscopy, X-ray diffraction or methods from non-linear optics such as sum frequency or second harmonic generation. For bridging the material gap, the strategy is to construct model systems, i.e. systems with reduced complexity compared to the real system but which still contain essential features of the real system. A good example is the microstructured planar Pt/YSZ catalysts displayed in Fig. 5 which are a model system of the Pt/YSZ catalyst with porous Pt electrodes.

The pressure gap and the special spillover species

All the UHV experiments on the mechanistic basis of electrochemical promotion have been conducted in a pressure range from 10^{-10}–10^{-4} mbar. Nearly all of the EPOC experiments have been conducted at high pressure in a range from 10^{-2} mbar to 1 bar. Typically, the reactants are in a pressure range 10^{-2}–10 mbar and the difference to atmospheric pressure is filled up with the carrier gas He. With exception of WF measurements with a Kelvin probe, no in situ methods have been applied in the EPOC experiments at high p. Evidently, a pressure gap of several orders of magnitude exists between the surface science-type studies and a typical EPOC experiment. What are the consequences of this pressure gap?

One conclusion of the surface science-type studies was that no special oxygen spillover species exists because the spillover species was shown to be identical with regular chemisorbed oxygen. In the light of the preceding discussion, one has to conclude that a negative result under UHV conditions does not rule out that a special spillover oxygen species might exist in EPOC experiments. A high oxygen pressure might stabilize an oxygen species which is unstable at low pressure. This argument is valid but to close the pressure gap, at least partially, in situ experiments with a differentially pumped so-called near ambient pressure (NAP) XP spectrometer were conducted that allowed to extend the pressure range to 0.2 mbar. Even under these conditions, the oxygen spillover species turned out to be identical with

oxygen chemisorbed from the gas phase as was shown for catalytic ethylene oxidation over a Pt/YSZ catalyst [27]. This finding still does not completely rule out the existence of a special oxygen spillover species at atmospheric pressure but the basis for still claiming the existence of such species has certainly become very small.

The puzzle of the non-Faradaicity of EPOC

The explanation of the non-Faradaicity of EPOC in the "sacrificial promoter mechanism" is based on the existence of a special spillover species. If this species does not exist, the mechanism breaks down. For solving the puzzle of the huge Λ-factors, we have to move into a branch of physics and chemistry called non-linear dynamics. Non-linear dynamics explains phenomena such as kinetic oscillations, chemical waves and other forms of self-organization [53]. The name has its origin in the requirement that the differential equations underlying these phenomena have to be non-linear.

In a bistable system, two stable states of the system coexist for identical parameters. Upon cyclic variation of the control parameter a hysteresis is observed. This is well known from magnetization of a ferromagnetic material but also in surface reactions bistability is frequently encountered [54]. Transitions between the two stable states proceed via propagating reaction fronts. Bistability can occur if one of the reactants can inhibit the adsorption of the other reactant. For example, in catalytic CO oxidation on Pt high CO coverages can inhibit the adsorption of oxygen [54]. Consequently, two states can coexist: an active state of the surface with a low CO coverage and an inactive state in which a high CO coverage blocks the adsorption of O_2. This type of behavior is illustrated in Fig. 9.

Here we consider catalytic ethylene oxidation on Pt/YSZ which due its record Λ-value of 3×10^5 plays a kind of paradigmatic role for EPOC. Ethylene at elevated temperatures decomposes easily on a Pt surface forming a graphitic-like carbonaceous film. The term "carbonaceous" simply means that, depending on temperature, decomposition of ethylene is not completed but that the graphitic film that is formed still may contain some hydrogen. The graphitic-like C-film inhibits O_2 adsorption thus poisoning the surface. As a consequence, the $C_2H_4+O_2$ reaction displays bistability as demonstrated by the rate curves in Fig. 10 [55] .

At low $p(C_2H_4)$ in the active state, the surface is oxygen covered and the rate rises linearly with $p(C_2H_4)$. Beyond a critical $p(C_2H_4)$ value indicated by the position of the rate maximum in Fig. 10, a graphitic-like C-film starts to develop and the rate drops to the low value of the inactive state. Upon cyclic variation of $p(C_2H_4)$, a hysteresis is observed as shown in Fig. 10. One notes two branches but different from the ideal case, the rate in the active state is still far below the value of the rate maximum. This deviation can be attributed to the heterogeneity of the surface, i.e. in the active state only part of the surface is freed of carbon.

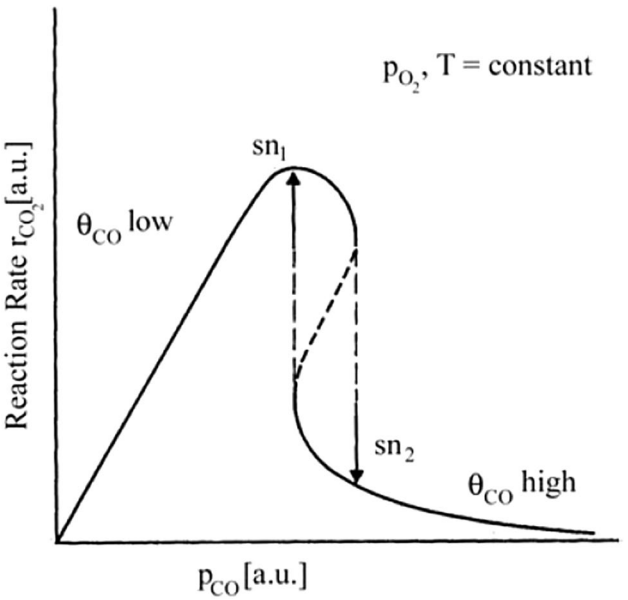

Fig. 9 Bistability in catalytic CO oxidation over Pt. In the region of bistability, two solutions of the kinetic equations coexist, a reactive state with a low CO coverage and an inactive state where a high CO coverage poisons the catalytic surface. Mathematically, the region of bistability is determined by two so-called saddle-node (sn) bifurcations [54]

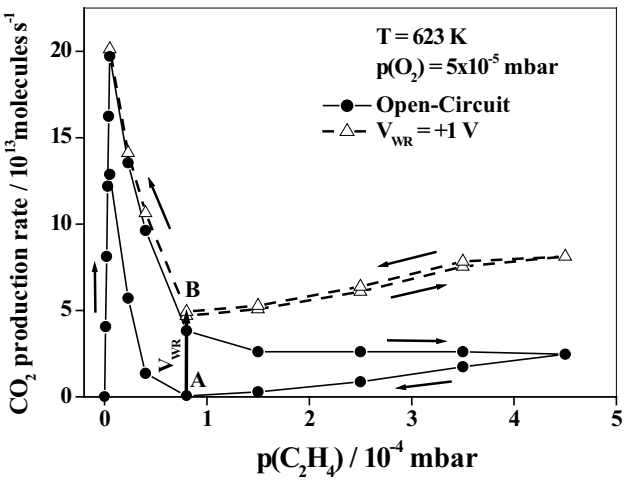

Fig. 10 Effect of electrochemical activation on the kinetics of ethylene oxidation on Pt/YSZ. The black circles mark the hysteresis obtained upon cycling $p(C_2H_4)$ under open-circuit conditions. The AB arrow indicates the rate increase as an electric potential $V_{WR}=1$ V is applied starting at point A. The triangles mark the reaction rate upon cycling $p(C_2H_4)$ with $V_{WR}=1$ V. Reaction conditions: $T=623$ K, $p(O_2)=5\times10^{-5}$ mbar. From ref. [55]

Starting from the low rate branch, upon electrochemical pumping with a positive potential, the rate undergoes a

transition to the active branch as indicated by an arrow in Fig. 10. The experiment demonstrates that the application of an electric potential can induce transitions from an inactive branch of the reaction to an active branch. This happens by a hole-eating mechanism demonstrated in an earlier experiment with a graphitized Pt/YSZ sample as displayed in Fig. 11 [32]. Spillover oxygen which reaches the Pt surface through small pores in the Pt layer reacts with carbon to CO and CO_2 thereby eating holes into the graphite layer. The same hole eating process will also take place during ethylene oxidation but now also oxygen is present in the gas phase. In the holes created by spillover oxygen, oxygen from the gas phase can adsorb and react thus enlarging the holes in an autocatalytic process. This causes the formation of reaction fronts.

The oxygen which is now required to burn the carbon is not oxygen from spillover but oxygen from the gas phase, i.e. the process is non-Faradaic. In terms of non-linear dynamics, the lower rate branch in the above example is metastable because it is only stabilized kinetically through the inhibitory effect of the graphite-like overlayer. The triggering of a transition from an inactive branch of the reaction to an active branch via an autocatalytic process is called "ignition". The decisive point is now the following. One can ask how big the perturbation has to be to ignite the system. The answer is, in principle infinitely small, but in reality a critical size of the hole has to be reached before the front can expand by itself [53].

Consider an analogy. If one has a barrel of fuel, then a small spark is sufficient to set this barrel on flame. Returning to EPOC, if the electrochemical current just ignites a system in a metastable state, the Λ-factor can, in principle, become infinitely large neglecting the limitation with the critical size. In the above example of catalytic ethylene oxidation in UHV, the Λ-factor is only about 4 which is far away from the 3×10^5 reported in the literature but at higher pressure additional factors come into play. In the example with the barrel of fuel, the ignition is a thermal ignition. The temperature rise by the reaction accelerates the reaction via Arrhenius law thus causing a positive feedback that results in a very rapid or even explosive burning of the fuel. In the above example with the two rate branches at 10^{-4} mbar, the ignition is clearly isothermal but the question is whether the reaction under typical EPOC conditions at much higher pressure is still isothermal?

One could expect that this question has already been answered experimentally, but, surprisingly, this aspect has been neglected completely in all EPOC experiments conducted so far. In catalytic CO oxidation on supported catalysts under reaction conditions in the mbar range, T-excursions of up to 100 K upon ignition have been reported [56]. In the $C_2H_4 + O_2$ reaction over Rh/SiO_2 catalysts, even T-increases of more than 200 K were seen [57]. Judging from catalytic CO oxidation, the pressure range where the reaction starts to become non-isothermal should be around 10^{-2} mbar which is just the pressure range where many EPOC experiments have been conducted. The p-limit where the reaction starts to become non-isothermal depends not only on the reaction but also on a number of experimental factors such as thermal conductivity and heat capacity of the sample, and whether an inert gas with good thermal conductivity such as He is present. YSZ as a ceramic material exhibits a low thermal conductivity but this may be counterbalanced by the high thermal conductivity of He. Clearly well-designed experiments are required to solve this question unambiguously.

In summary, the ignition mechanism has the advantage that one can explain the non-Faradaicity of the reaction without having to evoke the presence of a special spillover species which is a hypothetical species because so far no valid proof for its existence has been presented. The huge Λ-factors reported for some cases are thus less puzzling than originally thought. They appear to be simply the result of preparing a special situation of a surface poisoned with some inhibitory adsorbate. Lifting this inhibitory effect by electrochemical ignition then gives rise to enormous Λ-factors. Support for this interpretation which stresses the role of preparation of the catalysts comes from the huge spread of different Λ-factors reported for the same system. These range from 188 to 3×10^5 for the same system, ethylene oxidation over Pt/YSZ, and similar conditions [58]. For an experimental proof of the thermal ignition mechanism, new experiments are required, for example, by infrared thermography, which shows directly the presence or absence of T-rises during electrochemical activation of catalytic reactions.

New topics

A number of intriguing effects related to EPOC shall be introduced here only very briefly.

Permanent EPOC effect

This observation of an activation of the catalyst which persists even after switching off the electrical potential has been called permanent EPOC effect [1, 4, 59]. The origin of this effect is not clear but one can suspect that the electrochemical activation either led to chemical or morphological changes in the catalyst. In heterogeneous catalysis, it is common knowledge that any catalytic reaction modifies a catalytic surface with the extent ranging from atomic-scale restructuring to real morphological changes

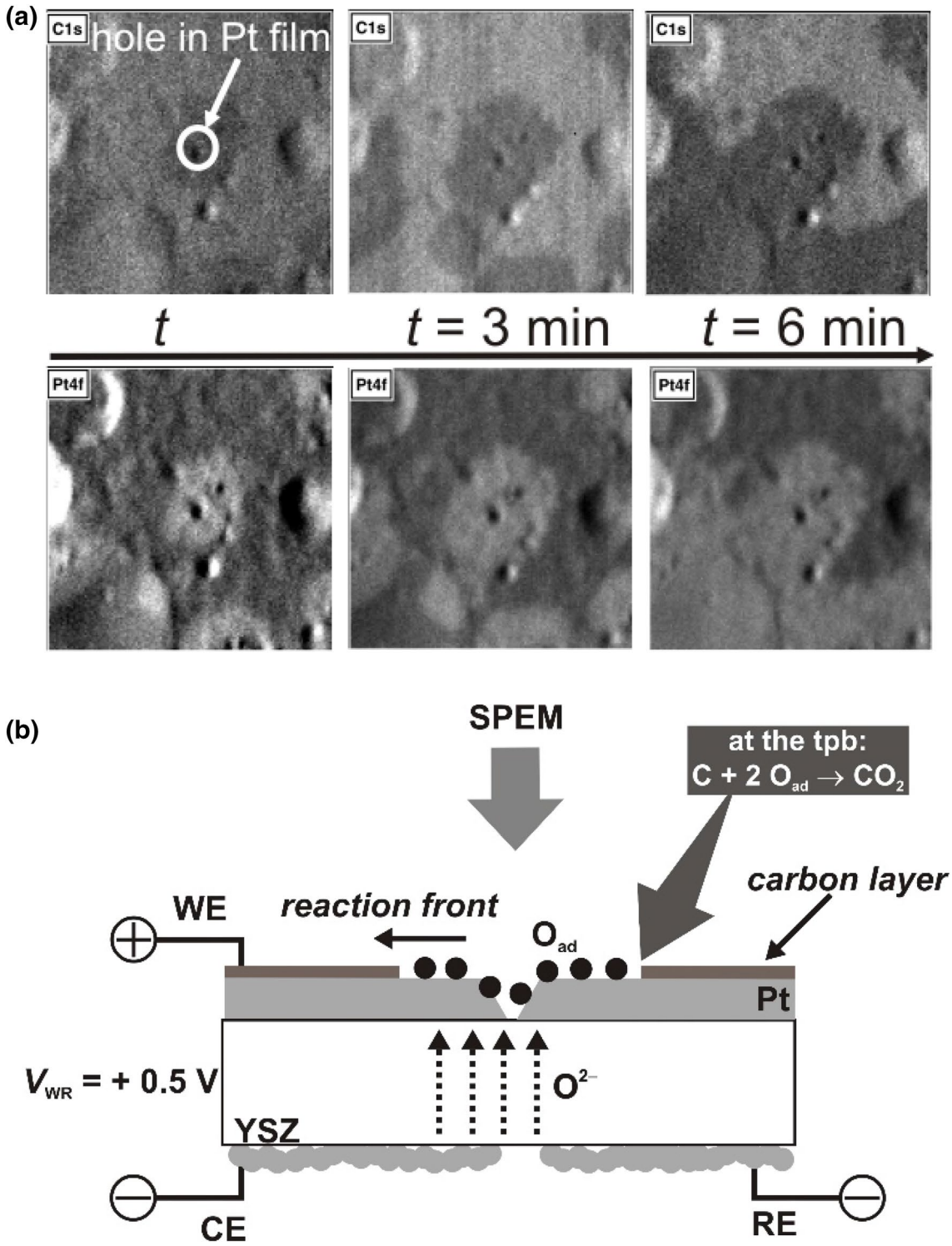

Fig. 11 Reaction of electrochemically generated spillover oxygen with carbon on a Pt/YSZ catalyst. **a** Scheme of the electrochemically controlled surface reaction experiment displayed in **b**. The working electrode is initially covered with carbon. Upon anodic polarization ($V_{WR} = +0.5$ V), oxygen spreads from a small hole in the electrode and reacts with the carbon layer forming a propagating reaction front. From ref. [32]. **b** Time sequence of SPEM images taken during anodic polarization ($V_{WR} = +0.5$ V). The lower row shows three Pt 4f maps, the upper row the corresponding C 1 s maps. From ref. [32]

of the catalyst. With respect to EPOC, an increase in the length of the tpb could, for example, explain an activation which persists after switching off the electric potential.

Indirect polarization

This represents a rather puzzling but with respect to applications also potentially interesting effect. As one applies an electric potential to noble metal electrodes on the surface of a solid electrolyte, one finds that also metal particles or metal stripes which are not electrically connected to the electrodes ("bipolar configuration") but are in their vicinity or in between them become activated though application of the potential [4, 60]. The nature of the effect has so far not been understood but since this effect could be used for an activation of nano-dispersed electrodes, the effect might be promising for future applications.

Conclusions and outlook

Summary

The EPOC effect has provided us with a wealth of intriguing and unexpected phenomena. The physical basis of EPOC is well established: it is the spillover of the transported species onto the surface of the metal electrodes. The driving force for this process is the raise of the chemical potential by the applied voltage, i.e. it is equilibrium thermodynamics. The EPOC effect connects several distinct areas, catalysis and surface science with electrochemistry and with materials science. The numerous phenomena in this area represent a challenge for both, fundamental science as well as for engineering practical applications.

Contribution of surface science

Under well-defined conditions, the surface analytical tools can be used to identify the relevant surface species and surface processes. The concept of electrochemically induced spillover of the transported species could be verified for the O^{2-}-conducting electrolyte YSZ as well as for the alkali ion-conducting β''-Al_2O_3 electrolyte.

These studies also showed that one also has to extremely careful in postulating a promotion mechanism without having the postulated species really having verified experimentally. The postulated special oxygen spillover species whose existence forms the basis of the "sacrificial promoter" mechanism has so far not been verified experimentally. Clearly, the only safe way to unravel a mechanism are in situ experiments identifying the surface species under the conditions of electrochemical promotion.

The puzzle of the huge non-Faradaicity

The somewhat puzzling large Λ-factors which may even be called mysterious by some are probably not mysterious at all. Instead of invoking a hypothetical special spillover species, the large Λ-factors can be explained as an ignition effect. Whether thermal ignition, i.e. a temperature rise caused by electrochemically igniting the reaction plays a role remains to be shown in future experiments.

Industrial applications

So far, despite some rather appealing aspects, the EPOC effect has found no practical applications in industry. The main obstacle is certainly that any practical application requires EPOC catalysts to be prepared in a reproducible and cost-effective way. Moreover, such a catalyst must be stable under reaction conditions for a sufficiently long time. The original way of depositing Pt paste with a brush led to highly active catalysts but this method is certainly not suitable for industrial applications. In the meantime, quite a number of new preparation methods including nano-dispersed electrodes have been developed but it remains to be shown which ones are suitable for practical applications.

Open questions

Although the physical basis of EPOC has been well established, the mechanisms of how the spillover species influence a particular catalytic reaction are almost completely speculative. With the upcoming new surface analytical in situ techniques, there should be good chances to resolve some of these problems in the near future. These methods should also allow to address questions like after the influence of the morphology of the Pt films on the electrocatalytic behavior and how the structure of the catalyst changes during electrochemical activation. In short, the pressure and materials gap still needs to be bridged for EPOC.

References

1. Vayenas CG, Bebelis S, Pliangos C, Brosda S, Tsiplakides D (2001) Electrochemical activation of catalysis: promotion, electrochemical promotion, and metal-support interactions. Kluwer Academic/Plenum Publishers, Dordrecht
2. Wagner C (1970) Adsorbed atomic species as intermediates in heterogeneous catalysis. Adv Catal 21:323–381
3. Vayenas CG, Bebelis S, Ladas S (1990) Dependence of catalytic rates on catalyst work function. Nature 343:625–627
4. Vernoux P, Lizarraga L, Tsampas MN, Sapountzi FM, Lucas-Consuegra AD, Valverde J-L, Vayenas SS,CG, Tsiplakides D, Balomenou S, Baranova EA (2013) Ionically conducting ceramics as active catalyst supports. Chem Rev 113:8192–8260

5. Vayenas CG, Promotion E (1996) Electrochem Soc Interface 5(4):34–37
6. Vayenas CG, Jaksic MM, Bebelis SI, Neophytides SG (1996) The electrochemical activation of catalytic reactions. Modern aspects of electrochemistry. Springer, New York, pp. 57–202
7. Wieckowski A, Savinova ER, Vayenas CG (2003) Catalysis and electrocatalysis at nanoparticle surfaces. Marcel Dekker, Inc., New York, 0-8247-0879-2
8. Vayenas CG, Koutsodontis CG (2008) Non-Faradaic electrochemical activation of catalysis. J Chem Phys 128(18):182506
9. Imbihl R (2010) Electrochemical promotion of catalytic reactions. Prog Surf Sci 85:241–278
10. Rickert H (1982) Electrochemistry of solids. Springer, Heidelberg
11. Lintz HG, Vayenas CG (1989) Solid electrolytes in heterogeneous catalysis. Angewandte Chemie Int Ed 28:708
12. Göpel W (1994) New materials and transducers for chemical sensors. Sens Actuators B 18:1–21
13. Bebelis S, Vayenas CG (1989) Non-Faradaic electrochemical modification of catalytic activity: 1. The case of ethylene oxidation on Pt. J Catal 118:125–146
14. Yentekakis IV, Neophytides S, Vayenas CG (1988) The effect of electrochemical O^{2-} pumping on the steady state and oscillatory behavior CO oxidation on polycrystalline Pt. J Catal 111:152–169
15. Bebelis S, Vayenas CG (1992) Non-faradaic electrochemical modification of catalytic activity. 6. Ethylene epoxidation on silver deposited on stabilized zirconia. J Catal 138(2):588–610
16. Marina OA, Yentekakis IV, Vayenas CG, Palermo A, Lambert RM (1997) In situ controlled promotion of catalyst surfaces via NEMCA: the effect of Na on the Pt-catalyzed NO reduction by H_2. J Catal 166(2):218–228
17. Yentekakis IV, Vayenas CG (1994) In-situ controlled promotion of Pt for CO oxidation via NEMCA using CaF_2 as the solid electrolyte. J Catal 149(1):238–242
18. Ploense L, Salazar M, Gurau B, Smotkin ES (1997) Proton spillover promoted isomerization of n-butylenes on Pd-black cathodes/Nafion 117. J Am Chem Soc 119(47):11550–11551
19. Christmann K (1991) Surface physical chemistry. Steinkopff, Darmstadt
20. Fleig J, Jamnik J (2005) Work function changes of polarized electrodes on solid electrolytes. J Electrochem Soc 152(4):E138–E145
21. Vayenas CG, Bebelis S, Yentekakis IV, Lintz HG (1992) Non-Faradaic electrochemical modification of catalytic activity: a status report. Catal Today 11(3):303–438
22. Bard AJ, Faulkner LR (2001) Electrochemical methods. Fundamentals and applications. Wiley, New York
23. Puglia C, Nilsson A, Hernnas B, Karis O, Bennich P, Martensson N (1995) Physisorbed, chemisorbed and dissociated O2 on Pt(111) studied by different core level spectroscopy methods. Surf Sci 342:119
24. Günther S, Kaulich B, Gregoratti L, Kiskinova M (2002) Photoelectron microscopy and applications in surface and materials science. Prog Surf Sci 70:187
25. Luerssen B, Günther S, Marbach H, Kiskinova M, Janek J, Imbihl R (2000) Photoelectron spectromicroscopy of electrochemically induced oxygen spillover at the Pt/YSZ interface. Chem Phys Lett 316(5–6):331–335
26. Ladas S, Kennou S, Bebelis S, Vayenas CG (1993) Origin of Non-Faradaic electrochemical modification of catalytic activity. J Phys Chem 97:8845–8848
27. Toghan A, Greiner M, Knop-Gericke A, Imbihl R (2018) Identification of the surface species in electrochemical promotion: ethylene oxidation over a Pt/YSZ catalyst. J Phys Chem C **(submitted)**
28. Katsaounis A, Nikopoulou Z, Verykios XE, Vayenas CG (2004) Comparative isotope-aided investigation of electrochemical promotion and metal-support interactions 1. $18O_2$ TPD of electropromoted Pt films deposited on YSZ and of dispersed Pt/YSZ catalysts. J Catal 222(1):192–206
29. Vayenas CG, Ioannides A, Bebelis S (1991) Solid electrolyte cyclic voltammetry for in situ investigation of catalyst surfaces. J Catal 129(1):67–87
30. Mutoro E, Luerssen B, Guenther S, Janek J (2009) The electrode model system $Pt(O_2)$/YSZ: influence of impurites and electrode morphology on cyclic voltammograms. Solid State Ion 180:1019–1033
31. Rotermund HH (1997) Imaging of dynamic processes on surfaces by light. Surf Sci Rep 29:265
32. Luerssen B, Mutoro E, Fischer H, Guenther S, Imbihl R, Janek J (2006) In situ imaging of electrochemically induced oxygen spillover on Pt/YSZ catalysts. Angew Chem Int Ed 45:1473–1476
33. Lewis R, Gomer R (1968) Adsorption of oxygen on platinum. Surf Sci 12:157
34. Wintterlin J, Schuster R, Ertl G (1996) Existence of a "Hot" Atom Mechanism for the Dissociation of O2 on Pt(111). Phys Rev Lett 77:123
35. Barth JV (2000) Transport of adsorbates at metal surfaces: from thermal migration to hot precursors. Surf Sci Rep 40:75–149
36. Mutoro E, Hellwig C, Luerssen B, Guenther S, Bessler WG, Janek J (2011) Electrochemically induced oxygen spillover and diffusion on Pt(111): PEEM imaging and kinetic modelling. PCCP 13:12798–12807
37. Vayenas CG, Archonta D, Tsiplakides D (2003) Scanning tunneling microscopy observation of the origin of electrochemical promotion and metal-support interactions. J Electroanal Chem 554–555:301–306
38. Mross WD (1983) Catalysis Rev Sci Eng 25:591
39. Bonzel HP, Bradshaw AM, Ertl G (eds) (1989) Physics and chemistry of alkali metal adsorption. Elsevier, Amsterdam
40. Kiskinova M (1992) Poisoning and promotion in catalysis based on surface science concepts. Elsevier, Amsterdam
41. Lambert RM (2003) Electrochemical and chemical promotion by alkalis with metal films and nanoparticles. In: Wieckowski A, Savinova ER, Vayenas CG (eds) Catalysis and electrocatalysis at nanoparticle surfaces. Marcel Dekker, Inc., New York, pp 583–611
42. Lambert RM, Palermo A, Williams FJ, Tikhov MS (2000) Electrochemical promotion of catalytic reactions using alkali ion conductors. Solid State Ion 136–137:677–685
43. Lambert RM, Williams FJ, Palermo A, Tikhov MS (2000) Modelling alkali promotion in heterogeneous catalysis: in situ electrochemical control of catalytic reactions. Top Catal 13:91–98
44. Williams FJ, Palermo A, Tikhov MS, Lambert RM (2000) Electrochemical promotion by sodium of the rhodium-catalyzed NO+CO reaction. J Phys Chem B 104(50):11883–11890
45. Williams FJ, Palermo A, Tracey S, Tikhov MS, Lambert RM (2002) Electrochemical promotion by potassium of the selective hydrogenation of acetylene on platinum: reaction studies and XP spectroscopy. J Phys Chem B 106(22):5668–5672
46. Janek J, Rohnke M, Luerßen B, Imbihl R (2000) Promotion of catalytic reactions by electrochemical polarization. Phys Chem Chem Phys 2:1935–1941
47. Pöpke H, Mutoro E, Raiß C, Luerßen B, Amati M, Abyaneh MK, Gregoratti L, Janek J (2011) The role of platinum oxide in the electrode system $Pt(O_2)$/yttria-stabilized zirconia. Electrochim Acta 56:10668–10675
48. Brosda S, Vayenas CG, Wei J (2006) Rules of chemical promotion. Appl Catal B 68(3–4):109–124
49. Nørskov JK, Abild-Pedersen F, Studt F, Bligaard T (2011) Density functional theory in surface chemistry and catalysis. Proc Natl Acad Sci USA 108:937

50. Schloegl R, Schoonmaker RC, Muhler M, Ertl G (1988) Bridging the "material gap" between single crystal studies and real catalysis. Catal Lett 1:237–242
51. Imbihl R, Behm RJ, Schlögl R (2006) Vom Idealen zum Realen System: Druck- und Material-Lücke in der Heterogenen Katalyse. Bunsenblätter 2:23–26
52. Prieto G, Schüth F (2015) Bridging the gap between insightful simplicity and successful complexity: from fundamental studies on model systems to technical catalysts. J Catal 328:59–71
53. Mikhailov AS (1991) Foundations of synergetics. Springer, Berlin
54. Imbihl R, Ertl G (1995) Oscillatory kinetics in heterogeneous catalysis. Chem Rev 95:697
55. Toghan A, Rösken LM, Imbihl R (2010) Origin of non-Faradayicity in electrochemical promotion of catalytic ethylene oxidation. PCCP 12:9811–9815
56. Kellow JC, Wolf EE (1990) Infrared thermography and FTIR studies of catalyst preparation effects on surface reaction dynamics during CO and ethylene oxidation on Rh/SiO_2 catalysts. Chem Eng Sci 45:2597–2602
57. Kellow JC, Wolf EE (1991) Propagation of oscillations during ethylene oxidation on a Rh/SiO_2 catalyst. AIChE J 37:1844–1848
58. Imbihl R, Toghan A (2011) Reply to comment by C. G. Vayenas, P. Vernoux. ChemPhysChem 12:1764
59. Nicole J, Comninellis C (1998) Electrochemical promotion of IrO_2 catalyst activity for the gas phase combustion of ethylene. J Appl Electrochem 28(3):223–226
60. Marwood M, Vayenas CG (1997) Electrochemical promotion of electronically isolated Pt catalysts on stabilized zirconia. J Catal 168(2):538–542